

**Photoproduction of  $J/\psi$  in association with a  $c\bar{c}$  pair**Rong Li<sup>1</sup> and Kuang-Ta Chao<sup>1,2</sup><sup>1</sup>*Department of Physics and State Key Laboratory of Nuclear Physics and Technology, Peking University, Beijing 100871, China*<sup>2</sup>*Center for High Energy Physics, Peking University, Beijing 100871, China*

(Received 10 April 2009; published 19 June 2009)

Based on the color-singlet model, we investigate the photoproduction of  $J/\psi$  associated with a  $c\bar{c}$  pair with all subprocesses including the direct, single-resolved, and double-resolved channels. The amplitude squared of these subprocesses are obtained analytically. By choosing corresponding parameters, we give theoretical predictions for the  $J/\psi$  transverse momentum and rapidity distributions both at the LEP II and at the future photon colliders for these subprocesses. The numerical results show that at the LEP II these processes cannot give enough contributions to account for the experimental data, and it indicates that the color-octet mechanism may still be needed. At the photon collider with the laser backscattering photons, the resolved photon channel will dominate over the direct one in small and moderate  $p_t$  regions with large  $\sqrt{s}$ . For their rapidity distribution with the laser backscattering photons, the resolved processes will be dominant in the whole region  $-2 < y < 2$ . By measuring the  $J/\psi$  production associated with a  $c\bar{c}$  pair, this process can be separated from the inclusive  $J/\psi$  production and may provide a new chance to test the color-singlet contributions.

DOI: 10.1103/PhysRevD.79.114020

PACS numbers: 12.38.Bx, 14.40.Lb

**I. INTRODUCTION**

Since the discovery of  $J/\psi$ , heavy quarkonium has provided an ideal laboratory to investigate the fundamental theory of strong interactions, quantum chromodynamics (QCD). Conventionally, people use the color-singlet model (CSM) [1] to describe the production and decay of heavy quarkonium. In order to overcome the theoretical difficulties related to the infrared divergences in the CSM [2,3] and reconcile the large discrepancy between the Tevatron data and the theoretical prediction given by the CSM [4], an effective theory, the nonrelativistic quantum chromodynamics (NRQCD) factorization formalism was proposed [5]. In NRQCD the production and decay rates of heavy quarkonium are factorized into the short distance parts and the long distance parts, and because the contributions of high Fock states are taken into account, the intermediate  $Q\bar{Q}$  pair that is produced in the short distance part can be in various states with different angular momenta and different colors. By introducing the color-octet mechanism (COM) in NRQCD, one may resolve the problem of infrared divergences in the CSM [6] and may hope to give a proper interpretation for the transverse momentum  $p_t$  distribution of  $J/\psi$  production at the Tevatron [7]. More detail descriptions on many aspects of heavy quarkonium physics can be found in Ref. [8].

The photoproduction of  $J/\psi$  has been investigated by many authors [9–11]. In 2001 the DELPHI Collaboration gave the measurement on inclusive photoproduction of  $J/\psi$  [12]. Theoretical analysis indicates that the  $p_t$  distribution predicted in the CSM is an order of magnitude smaller than the experimental result and the NRQCD prediction can give a good account for it by the COM [13]. It has been viewed as a strong support to the COM

in NRQCD. The color evaporation model and the  $k_t$  factorization formalism were also used to investigate this process [14]. Furthermore, the next-to-leading order (NLO) QCD corrections to the processes  $\gamma + \gamma \rightarrow c\bar{c}[{}^3S_1^{(8)}] + g$  and  $\gamma + \gamma \rightarrow c\bar{c}[{}^3S_1^{(1)}] + \gamma$  are accomplished in [15] and the authors also give theoretical predictions for these processes at the TESLA.

Recently, a number of studies show the importance of the heavy quark pair associated  $J/\psi$  production in the CSM. The contributions from  $J/\psi + c + \bar{c}$  final states in  $J/\psi$  inclusive production have been discussed by many authors at  $B$  factories [16,17] and LEP [18], and at the Tevatron and LHC [11,19], and have even been studied in the  $k_t$  factorization formalism [20]. The  $J/\psi + c + \bar{c}$  as final states in the  $\gamma N$  collision were studied a long time ago [21]. Although it is a NLO process, the  $p_t$  distribution can be changed and the differential cross section can be enhanced at large  $p_t$  due to the different kinematics of the Feynman diagrams. At  $B$  factories, the  $e^+ + e^- \rightarrow J/\psi + c + \bar{c}$  process gives more than half the contribution to the total cross section of the  $J/\psi$  inclusive production [22]. In Ref. [18], the authors study the process  $\gamma + \gamma \rightarrow J/\psi + c + \bar{c}$  and find that the NLO process gives more contribution compared with that of the leading-order (LO) process  $\gamma + \gamma \rightarrow J/\psi + \gamma$  at the LEP. In the large  $p_t$  region, the contribution from  $\gamma + \gamma \rightarrow J/\psi + c + \bar{c}$  is bigger than that of the fragmentation process  $\gamma + \gamma \rightarrow c + \bar{c} \text{ frag} \rightarrow J/\psi + c + \bar{c}$ . In Ref. [20], the process  $\gamma + g \rightarrow J/\psi + c + \bar{c}$  was studied in the  $k_t$  factorization formalism.

In this paper, we will investigate all the subprocesses of the photoproduction of  $J/\psi$  associated with  $c\bar{c}$  in the CSM. First, the full results including contributions from all the single and double-resolved photon processes of the  $J/\psi$  production associated with the heavy quark-antiquark

pair at the LEP will be presented for the first time. Second, these processes will be extended to the photon colliders and the results with different photon production mechanisms will be given.

The paper is organized as follows. In Sec. II, we give definitions of some relevant quantities and derive the analytical formulas of the differential cross sections for all the subprocesses. Numerical results are given in Sec. III. Finally, a summary is given in Sec. IV.

## II. FORMULATION AND CALCULATION

There are three classes of subprocesses for  $\gamma + \gamma \rightarrow J/\psi + c + \bar{c} + X$ : As shown in Eq. (1), the direct process, where the two photons directly couple to the final heavy quarks; In Eq. (2), the single-resolved process, where one photon fluctuates to a parton (here, the gluon) and collides with the other photon to produce the final states; In Eq. (3), the double-resolved processes, where both the two photons fluctuate to partons to produce the final states. So in order to investigate the process thoroughly, the following four

subprocesses must be calculated:

$$\gamma + \gamma \rightarrow J/\psi + c + \bar{c}, \quad (1)$$

$$\gamma + g \rightarrow J/\psi + c + \bar{c}, \quad (2)$$

$$g + g \rightarrow J/\psi + c + \bar{c}, \quad q + \bar{q} \rightarrow J/\psi + c + \bar{c}. \quad (3)$$

The four subprocesses involve 20, 30, 42, 7 Feynman diagrams, respectively. Figures 1 and 2 just show the Feynman diagrams of the processes  $\gamma + g \rightarrow J/\psi + c + \bar{c}$  and  $q + \bar{q} \rightarrow J/\psi + c + \bar{c}$ . The Feynman diagrams of the other two subprocesses are the same as those given in the Res. [18,19]. In the Feynman diagrams the generated two charm quarks and two anticharm quarks can combine into a bound state charmonium with another charm quark pair. Here all combinations are allowed as long as the charmonium is in a color-singlet state. Following the color-singlet factorization formalism and the standard covariant projection method [23], the scattering amplitudes of these subprocesses can be expressed as

$$\begin{aligned} \mathcal{M}(a(k_1) + b(k_2) \rightarrow c\bar{c}(^{2S+1}L_J^{(1)})(P) + c(p_1) + \bar{c}(p_2)) \\ = \sqrt{C_L} \sum_{L_z S_z} \sum_{s_1 s_2} \sum_{jk} \langle s_1; s_2 | SS_z \rangle \langle LL_z; SS_z | JJ_z \rangle \langle 3j; \bar{3}k | 1 \rangle \mathcal{M}(a(k_1) + b(k_2) \\ \rightarrow c_j\left(\frac{P}{2}; s_1\right) + \bar{c}_k\left(\frac{P}{2}; s_2\right) + c(p_1) + \bar{c}(p_2)), \end{aligned} \quad (4)$$

where  $\langle 3j; \bar{3}k | 1 \rangle$ ,  $\langle s_1; s_2 | SS_z \rangle$ , and  $\langle LL_z; SS_z | JJ_z \rangle$  are the color-SU(3), spin-SU(2), and orbital angular momentum Clebsch-Gordan coefficients, respectively, for  $c\bar{c}$  pairs projecting out appropriate quantum numbers of the bound states. The  $C_L$  is the probability that describes a heavy quark-antiquark pair having the appropriate quantum numbers to evolve into a corresponding meson and, for the  $J/\psi$

here, can be related to the wave function at the origin  $R(0)$  or the color-singlet long distance matrix element  $\langle 0 | O_1^{J/\psi} | 0 \rangle$  as follows:

$$C_L = \frac{1}{4\pi} |R(0)|^2 = \frac{1}{2N_c(2J+1)} \langle 0 | O_1^{J/\psi} | 0 \rangle. \quad (5)$$

As for  $J/\psi$  production, the spin-triplet projection operator

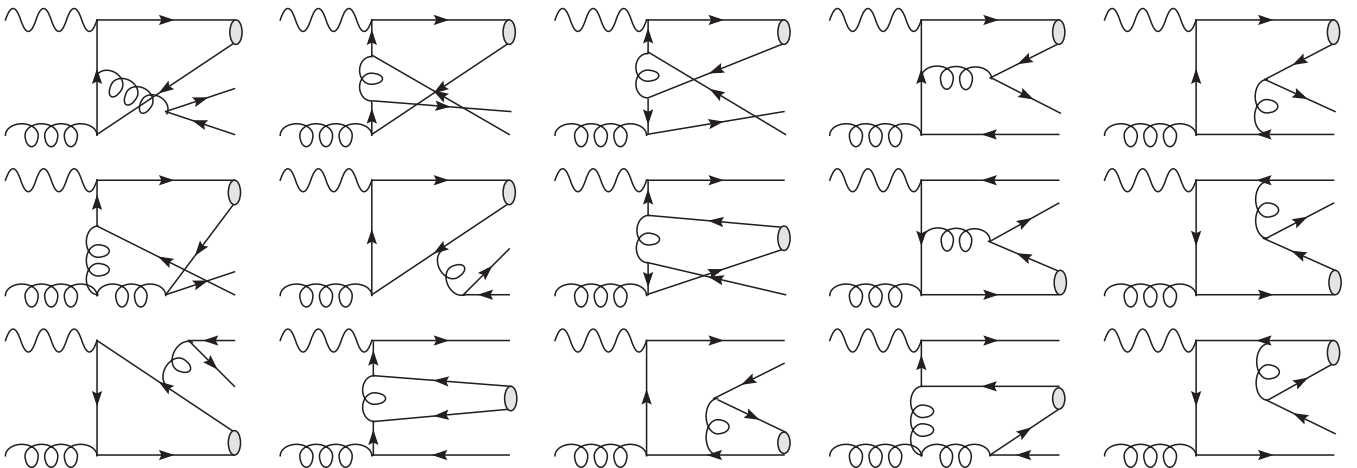


FIG. 1. Typical Feynman diagrams for subprocesses  $\gamma + g \rightarrow J/\psi + c + \bar{c}$ . The others can be obtained by reversing the fermion lines.

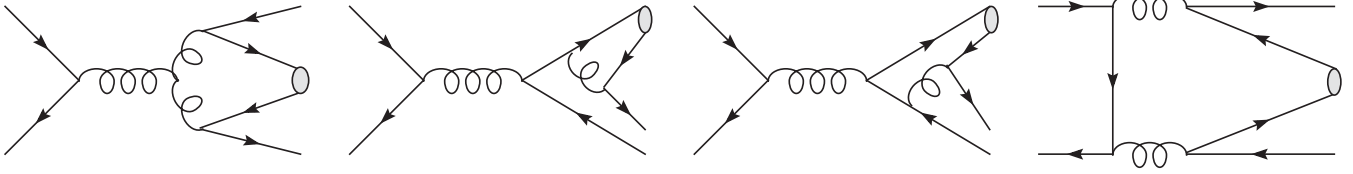


FIG. 2. Typical Feynman diagrams for subprocesses  $q + \bar{q} \rightarrow J/\psi + c + \bar{c}$ . The others can be obtained by reversing the fermion lines.

should be used, which is defined as

$$P_{1S_z}(P, 0) = \sum_{(1/2)(1/2)} \left\langle \frac{1}{2}; \frac{1}{2} \mid 1S_z \right\rangle v\left(\frac{P}{2}; \frac{1}{2}\right) \bar{u}\left(\frac{P}{2}; \frac{1}{2}\right) \\ = \frac{1}{2\sqrt{2}} \not{\epsilon}(S_z)(\not{P} + 2m_c). \quad (6)$$

At the same time, the color projection operator for the color-singlet state is given by

$$\langle 3j; \bar{3}k \mid 1 \rangle = \delta_{jk} / \sqrt{N_c}. \quad (7)$$

Technically, we use the FeynArts [24] to generate the Feynman diagrams and amplitudes for the subprocesses  $a(k_1) + b(k_2) \rightarrow c_j(\frac{P}{2}; s_1) + \bar{c}_k(\frac{P}{2}; s_2) + c(p_1) + \bar{c}(p_2)$  in the Feynman gauge, then insert the projection operator

$$\frac{\bar{v}(\frac{P}{2}; s_2) \not{\epsilon}(S_z) u(\frac{P}{2}; s_1)}{2\sqrt{2}M_c} \quad (8)$$

to project the  $c\bar{c}$  pair onto a  $^3S_1$  state. The FeynCalc [25] is used to evaluate the square of the amplitudes. In calculating the subprocesses  $g + g \rightarrow J/\psi + c + \bar{c}$ ,  $-g^{\mu\nu}$  is used for the polarization summation of the initial gluons and therefore the corresponding contribution of the ghost diagrams must be subtracted. The analytical results for every subprocess are too tedious to be shown in this paper. In order to check the gauge invariance, the polarization vector of one initial gluon (photon) is replaced by the corresponding momentum in the direct and single-resolved processes and the zero results are obtained at the level of squared matrix element analytically. To check the gauge invariance of the subprocess  $g + g \rightarrow J/\psi + c + \bar{c}$ , we replace the polarization vector of one of the initial gluons by its momentum and use the physical polarization tensor  $P_{\mu\nu}$  for the polarization summation of the other gluon. Then the square of the amplitude vanishes. Otherwise, the ghost diagrams must be taken into consideration for checking the gauge invariance. Here the physical polarization tensor  $P_{\mu\nu}$  is explicitly expressed as

$$P_{\mu\nu} = -g_{\mu\nu} + \frac{k_\mu \eta_\nu + k_\nu \eta_\mu}{k \cdot \eta}, \quad (9)$$

where  $k$  is the momentum of the gluon,  $\eta$  is an arbitrary lightlike four vector with  $k \cdot \eta \neq 0$ . In the calculation,  $\eta$  is set as the momentum of the other initial gluon conveniently.

The differential cross section can be obtained by convoluting the parton level differential cross section with the photon density functions and the parton distribution functions of the photon. It is expressed as

$$d\sigma(e^+ + e^- \rightarrow e^+ + e^- + J/\psi + c + \bar{c}) \\ = \int dx_1 dx_2 f_\gamma(x_1) f_\gamma(x_2) \sum_{i,j} \int dx_i dx_j f_{i/\gamma}(x_i) \\ \times f_{j/\gamma}(x_j) d\hat{\sigma}(i + j \rightarrow J/\psi + c + \bar{c}), \quad (10)$$

where  $f_\gamma(x)$  is the photon density function and  $f_{i/\gamma}(x)$  is the parton distribution function of the photon. Here the labels  $i$  and  $j$  denote the parton contents of the photon, such as gluon and the light quarks. In the direct photon process, the distribution function  $f_{\gamma/\gamma}(x) = \delta(1-x)$ .

In the photon-photon collisions, the initial photons can be generated by the bremsstrahlung or by the laser backscattering (LBS) from the  $e^+e^-$  collision. The spectrum of the bremsstrahlung photon can be described by the Weizsacker-Williams approximation (WWA) as follows [26]:

$$f_\gamma(x) = \frac{\alpha}{2\pi} \left( 2m_e^2 \left( \frac{1}{Q_{\max}^2} - \frac{1}{Q_{\min}^2} \right) x \right. \\ \left. + \frac{(1 + (1-x)^2)}{x} \log\left(\frac{Q_{\max}^2}{Q_{\min}^2}\right) \right), \quad (11)$$

where  $x = E_\gamma/E_e$ ,  $\alpha$  is the fine structure constant and  $m_e$  is the electron mass. The definitions of  $Q_{\max}^2$  and  $Q_{\min}^2$  are given by

$$Q_{\min}^2 = \frac{m_e^2 x^2}{1-x}, \quad (12)$$

$$Q_{\max}^2 = \left( \frac{\sqrt{s}\theta}{2} \right)^2 (1-x) + Q_{\min}^2, \quad (13)$$

where  $\theta$  is the angle between the momentum of the photon and the direction of the electron beam. This angle is taken as 32 mrad at the LEP II. On the other hand, the laser backscattering can generate more energetic and luminous photons. The spectrum of the LBS photon is expressed as [27]

$$f_\gamma(x) = \frac{1}{N} \left[ 1 - x + \frac{1}{1-x} - 4r(1-r) \right], \quad (14)$$

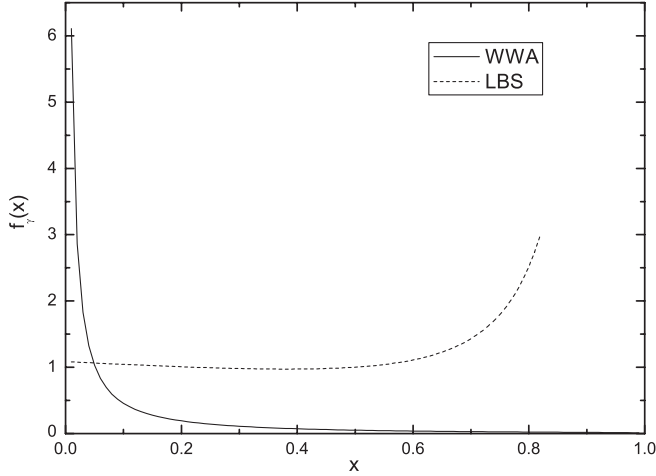


FIG. 3. The photon spectra of the WWA and LBS at  $\sqrt{s} = 500$  GeV.

where  $x = E_\gamma/E_e$ ,  $r = \frac{x}{x_m(1-x)}$ , and the constant  $N$  is given by

$$N = \left(1 - \frac{4}{x_m} - \frac{8}{x_m^2}\right) \log(1 + x_m) + \frac{1}{2} + \frac{8}{x_m} - \frac{1}{2(1 + m_x)^2}, \quad (15)$$

where  $x_m = 4E_b E_l \cos^2 \frac{\theta}{2}$ . Here  $E_b$  is the energy of the electron beam,  $E_l$  is the energy of the incident laser beam, and  $\theta$  is the angle between the laser and the electron beam. The energy of the LBS photon is restricted by the following equation:

$$0 \leq x \leq \frac{x_m}{1 + x_m}, \quad (16)$$

Telnov [28] argued that the optimal value of  $x_m$  is 4.83.

The spectra of the LBS and WWA photons are very different. While the latter depends only on the center-of-mass energy, the former depends on the parameter  $x_m$  also. By comparing the spectra of the WWA photon at  $\sqrt{s} = 500$  GeV to the one at  $\sqrt{s} = 1$  TeV, we clearly see that there is no qualitative difference between them and the numerical difference is less than 15%. Therefore, we just show the comparison of the spectra of WWA photon and that of the LBS photon at  $\sqrt{s} = 500$  GeV in Fig. 3. And it can be seen that the distribution of the WWA photon is large at the small  $x$  region and tends to infinite at the end point  $x \approx 0$ . On the contrary, the distribution of the LBS photon is moderate in the whole  $x$  region and get its maximum value at the largest  $x$  point. These two distributions can result in significant different results.

### III. NUMERICAL RESULTS AND DISCUSSIONS

In calculating the numerical results, we choose the following parameters:  $M_c = 1.5$  GeV,  $\alpha = 1/137$ ,  $m_e =$

0.511 MeV, and the color-singlet matrix element  $\langle 0 | \mathcal{O}^{J/\psi}({}^3S_1^{[1]}) | 0 \rangle = 1.4$  GeV<sup>3</sup> [18]. The GRS99 [29] parton distribution function of photon is used and the running of  $\alpha_s$  is evaluated by the LO formula of GRV98 [30]. Both the renormalization and factorization scales are fixed as  $\sqrt{4M_c^2 + p_t^2}$ . Aside from the direct production of  $J/\psi$  we should also include the feeddown contribution from the production of  $\psi'$  followed by the decay  $\psi' \rightarrow J/\psi + X$  by multiplying the numerical results of  $J/\psi$  by a factor of 1.278, which comes from the ratio of leptonic decay widths of  $\psi'$  to  $J/\psi$  and the branching fraction of decay  $\psi' \rightarrow J/\psi + X$  (see, e.g. Ref. [18]).

The differential cross sections  $d\sigma/dp_t^2$  and the rapidity distributions for all the four subprocesses at the LEP II are shown in Fig. 4. To obtain theoretical predictions, the parameters which are related to the LEP II experimental conditions are chosen as  $\sqrt{s} = 197$  GeV,  $\theta_{\max} = 32$  mrad and the rapidity cut  $-2 < y < 2$ . The constraint of center-of-mass energy for the two photons is  $W \leq 35$  GeV [12]. From Fig. 4, one can see that the direct photon subprocess is dominant at the LEP II with the WWA photon. The contribution from the single-resolved subprocess is smaller than that of the direct one by an order or more in magnitude and the contributions from the double-resolved subprocesses are even smaller than that of the direct one by almost four orders or more in magnitude. It also can be seen that the contribution from the quark-antiquark subprocess is larger than that of the double-resolved gluon subprocess.

In the future, the  $e^+e^-$  collider may run at  $\sqrt{s} = 500$  GeV or even at  $\sqrt{s} = 1$  TeV, and the LBS photon collision may be realized. Therefore, we also investigate the four subprocesses at  $\sqrt{s} = 500$  GeV and  $\sqrt{s} = 1$  TeV. For comparison, we give the theoretical results with both the WWA photon and LBS photon at these two center-of-mass energies. Here we set the  $\theta_{\max}$  of the WW approximation as 20 mrad [10] and the  $x_m$  of the LBS photon as 4.83, which determines the maximum photon energy fraction as 0.83 [28]. In contrast to the calculation for the LEP II, here we do not use the constrain  $W \leq 35$  GeV.

Figures 5 and 6 give the  $p_t$  distributions of the differential cross sections and the rapidity distributions at different center-of-mass energies with the WWA photon and the LBS photon, respectively, at the photon collider. For the WWA photon case, the direct photon production subprocess is always the dominant one. The contribution from the single-resolved process is less than that from the direct one, but larger than those from the double-resolved processes. However, in the case of the LBS photon, with the increase of the center-of-mass energy, the contributions from the single-resolved and the double-resolved gluon subprocesses are compatible with or even larger than that from the direct one. But the contribution from the quark-antiquark subprocess is much smaller than those from the other three subprocesses.

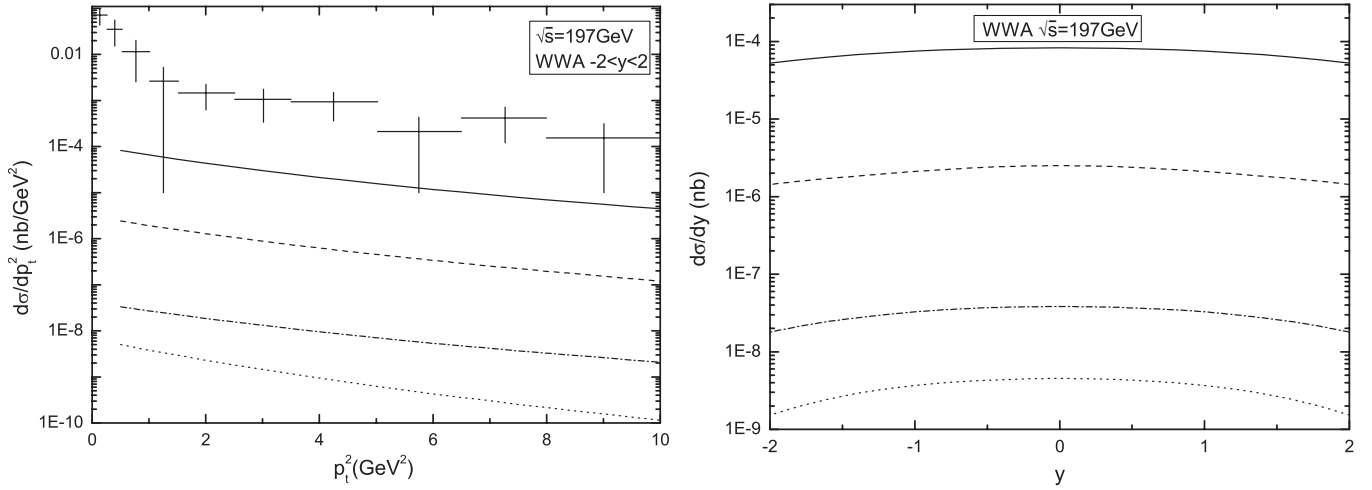


FIG. 4.  $p_T$  and rapidity distributions of cross sections of  $J/\psi + c + \bar{c}$  production in various subprocesses at the LEP II. The solid, dashed, dotted, and dash-dotted lines correspond to the subprocesses  $\gamma + \gamma \rightarrow J/\psi + c + \bar{c}$ ,  $\gamma + g \rightarrow J/\psi + c + \bar{c}$ ,  $g + g \rightarrow J/\psi + c + \bar{c}$ , and  $q + \bar{q} \rightarrow J/\psi + c + \bar{c}$ , respectively. The experimental result of DELPHI for the  $p_T$  distribution of  $J/\psi + X$  is also presented [12].

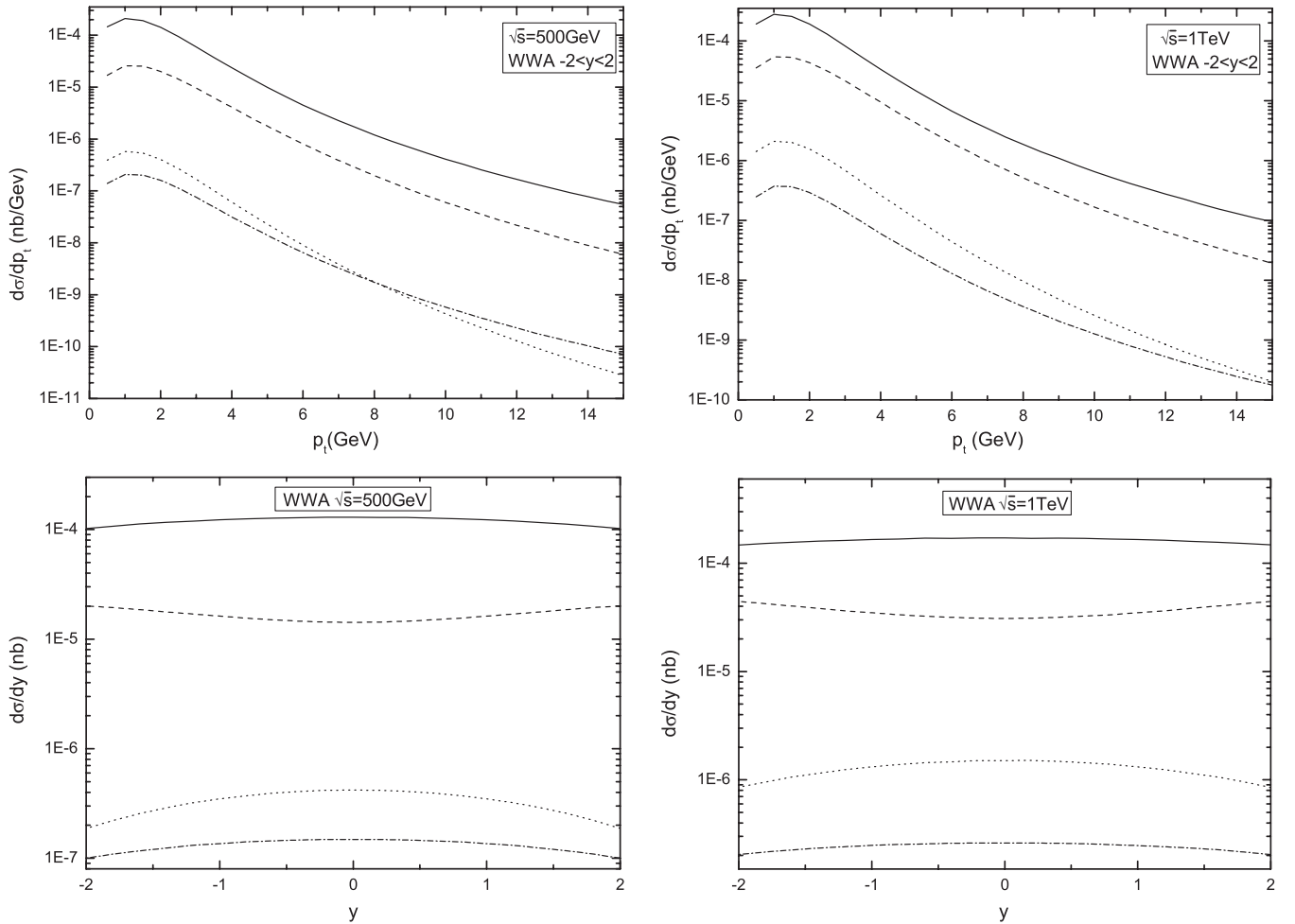


FIG. 5.  $p_T$  and rapidity distributions of differential cross sections of  $J/\psi + c + \bar{c}$  production at the photon collider with the WWA photon spectrum at different  $\sqrt{s}$ . Here we use the same notations as those in Fig. 4.



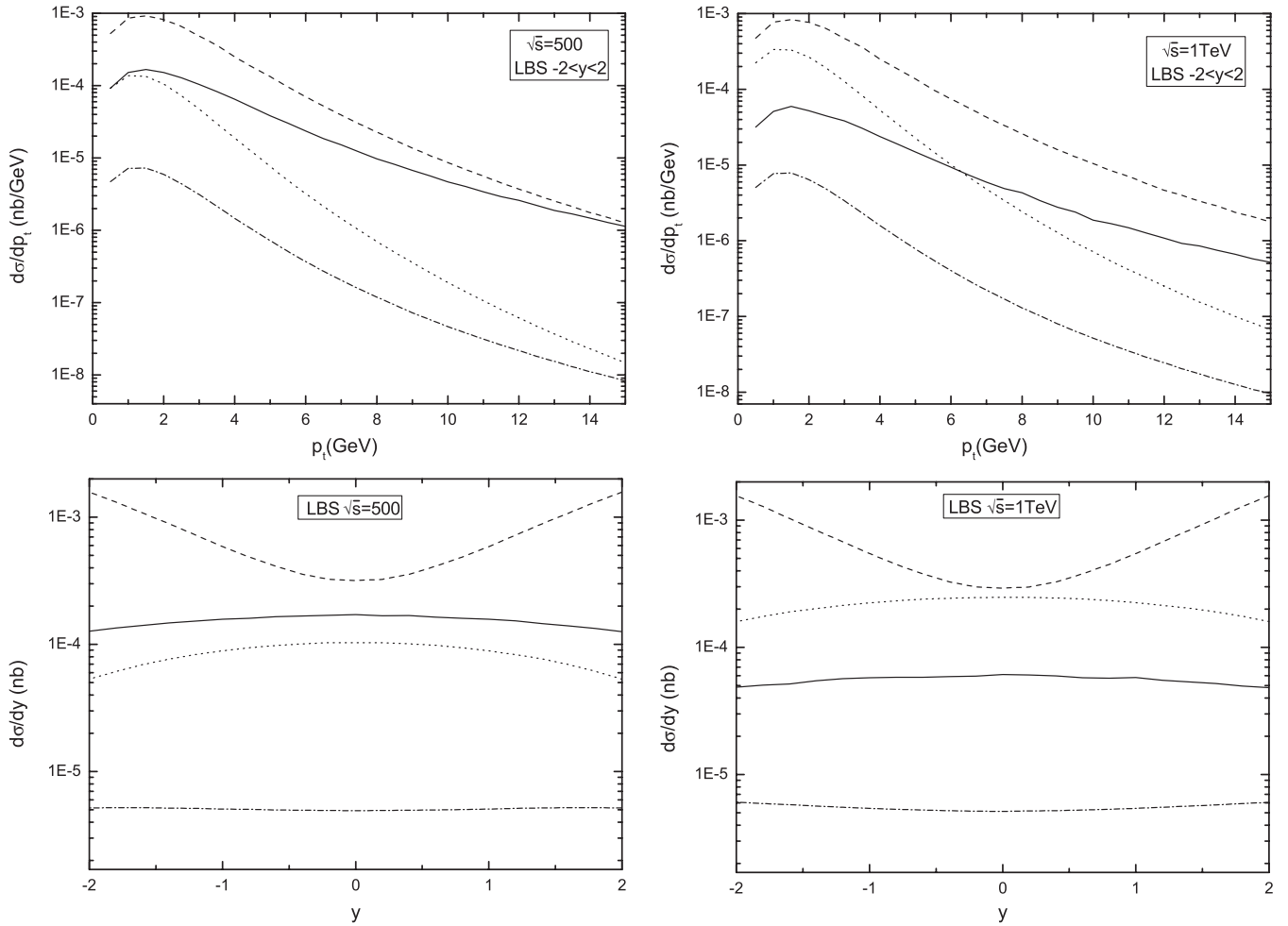


FIG. 6.  $p_t$  and rapidity distributions of differential cross sections of  $J/\psi + c + \bar{c}$  production at the photon collider with the LBS photon spectrum at different  $\sqrt{s}$ . Here we use the same notations as those in Fig. 4.

Figure 7 shows the parton distributions of photon in the GRS99 parametrization [29]. It can be seen that the gluon content is dominant in the small  $x$  region and even divergent when  $x$  tends to zero. It is only in the large  $x$  region that the quark contents can be dominant.

Let us first consider the subprocesses with the LBS photons as initial states. When the  $p_t$  of  $J/\psi$  is lower or the  $\sqrt{s}$  becomes larger, the contributions from small  $x$  region partons are dominant. Because the LBS photon spectrum function has no singularity at the small  $x$  region, and at the same time the gluon distribution function of the photon has a great enhancement at the small  $x$  region, the single-resolved and double-resolved gluon subprocess can be dominant in the  $J/\psi$  production with lower  $p_t$  or larger  $\sqrt{s}$ . It also can be seen that the contribution of the single-resolved subprocess is small in the midrapidity region and large in the forward and backward region in Fig. 6 with the LBS photons. This is because, in the forward and backward region the main contribution comes from the collision of a large momentum photon and a small momentum gluon in the small  $x$  region with an enhanced parton distribution

function of the resolved photon. However, as for the subprocesses with the WWA photons as initial states, where both the photon spectrum function and the gluon distribu-

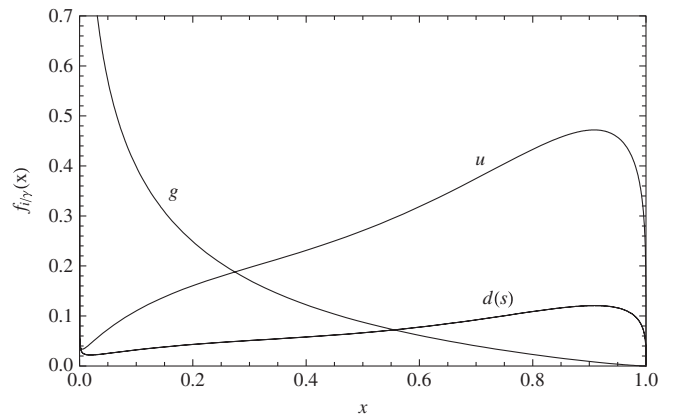


FIG. 7. Parton distributions of the photon in the GRS99 [29] parametrization at  $Q^2 = 30 \text{ GeV}^2$ . Here  $x$  is the parton energy fraction.

TABLE I. Integrated cross sections of photoproduction of  $J/\psi$  associated with a  $c\bar{c}$  pair for different initial state  $e^+e^-$  energy  $\sqrt{s}$  and subprocesses. The  $p_t$  cut of  $J/\psi$  is set as  $p_t > 1$  GeV. Other parameters and cut conditions are chosen as the one being used to calculate the  $p_t$  distributions in the text. (Units:  $\sqrt{s}$  in GeV and  $\sigma$  in nb.)

$\sqrt{s}$	$\sigma_{\gamma+\gamma}$	$\sigma_{\gamma+g}$	$\sigma_{g+g}$	$\sigma_{q+\bar{q}}$
197(WWA)	$2.06 \times 10^{-4}$	$5.82 \times 10^{-6}$	$8.68 \times 10^{-9}$	$9.07 \times 10^{-8}$
500(WWA)	$3.51 \times 10^{-4}$	$5.06 \times 10^{-5}$	$9.74 \times 10^{-7}$	$4.02 \times 10^{-7}$
500(LBS)	$5.33 \times 10^{-4}$	$2.34 \times 10^{-3}$	$2.57 \times 10^{-4}$	$1.82 \times 10^{-4}$
1000(WWA)	$4.80 \times 10^{-4}$	$1.11 \times 10^{-4}$	$3.80 \times 10^{-6}$	$7.42 \times 10^{-7}$
1000(LBS)	$1.97 \times 10^{-4}$	$2.26 \times 10^{-3}$	$6.66 \times 10^{-4}$	$1.72 \times 10^{-5}$

tion function of the photon are greatly enhanced at the small  $x$  region, the single- and double-resolved subprocesses have no predominance compared with the direct one. In the large  $x$  region the distributions of quarks are larger than that of the gluon in the resolved photon. Because of the constraint on  $\sqrt{s}$  of photons  $W_{\gamma\gamma} < 35$  GeV at LEP II, the partons with large  $x$  will be the dominant ones, which makes the contribution from the quark-antiquark process larger than that of the double-resolved gluon one as shown in Fig. 4.

Table I gives the integrated cross sections of every subprocess of the photoproduction of  $J/\psi$  associated with the  $c\bar{c}$  pair. From the numerical results, it can be seen that the total contributions from the resolved (including single and double-resolved) subprocesses are smaller than that of the direct one by about an order of magnitude in the case of WWA photons. On the contrary, in the case of LBS photons the total contributions from the resolved subprocesses are larger than that from the direct one by a factor of 5.2 at  $\sqrt{s} = 500$  GeV and 15 at  $\sqrt{s} = 1000$  GeV. It can also be inferred from the  $p_t$  or rapidity distribution presented in Figs. 4–6. At the same time, all the integrated cross sections increase with the increase of  $\sqrt{s}$  for the processes initiated by the WWA photons. And in the case of LBS photons, only the cross section of the subprocess  $g + g \rightarrow J/\psi + c\bar{c}$  increased with  $\sqrt{s}$  enhanced from 500 GeV to 1 TeV.

For the direct photon subprocess, our numerical result is different [31] from the one in Ref. [18]. The numerical results indicate that the contributions from the single-resolved and double-resolved processes are much less than that from the direct one at the LEP II. The authors of Ref. [15] have given the results of the NLO QCD corrections for the subprocesses  $\gamma + \gamma \rightarrow J/\psi + \gamma$  and  $\gamma + \gamma \rightarrow c\bar{c}[{}^3S_8^1] + g$  at the TESLA. For the subprocess  $\gamma + \gamma \rightarrow J/\psi + \gamma$ , the  $K$  factor is smaller than 1. And the QCD correction for the color-octet subprocess  $\gamma + \gamma \rightarrow c\bar{c}[{}^3S_8^1] + g$  can enhance the differential cross section significantly in the large  $p_t$  region. From the above NLO results at the TESLA, one can expect that the NLO corrections to the color-singlet subprocess  $\gamma + \gamma \rightarrow J/\psi + \gamma$  could not enhance the result largely at the LEP II also. So the contributions from the color-octet mechanism cannot be excluded in the inclusive  $J/\psi$  photoproduction at the

LEP II. The full investigation on the NLO QCD radiative corrections on the direct and resolved subprocesses may help us to clarify the situation.

As for the photon collider with the LBS initial photons, the contributions from the single- and double-resolved photon subprocesses become significantly large as  $\sqrt{s}$  increases in the low and moderate  $p_t$  region and in the rapidity distribution. This feature comes from the small  $x$  behavior of the gluon distribution function of the photon, and can be tested in future experiments.

#### IV. SUMMARY

In this paper, we investigate the production of  $J/\psi$  associated with a  $c\bar{c}$  pair in the CSM in photon-photon collisions, including the direct, single-resolved, and double-resolved subprocesses. The formulas for the cross sections of the four subprocesses are obtained in the collinear factorization formalism. Moreover, the results of the single-resolved subprocess are given for the first time. The numerical results show that the contributions from color-octet processes cannot be excluded at present with the LEP experiment.

At the photon collider with the LBS initial photons, the single-resolved and even the double-resolved processes will dominate over the direct one in the rapidity distribution or the  $p_t$  distribution with small and moderate  $p_t$ . By measuring the final state  $J/\psi$  and  $c\bar{c}$  pair, the process  $\gamma + \gamma \rightarrow J/\psi + c + \bar{c} + X$  can be separated from the inclusive  $J/\psi$  production and could provide a channel to probe the parton contents of the photon. Furthermore, to separate this channel in experiment and compare the data with the theoretical prediction in the CSM also gives a new chance to test the CSM contributions.

#### ACKNOWLEDGMENTS

We thank Professor Jian-Xiong Wang, Dr. Ce Meng, and Dr. Yu-Jie Zhang for helpful discussions. R. L. also thanks Dr. E. Reya and Dr. I. Schienbein for providing the FORTRAN code on the GRS parton distribution of the photon. This work was supported by the National Natural Science Foundation of China (No. 10675003, No 10721063).

- [1] M.B. Einhorn and S.D. Ellis, Phys. Rev. D **12**, 2007 (1975); S.D. Ellis, M.B. Einhorn, and C. Quigg, Phys. Rev. Lett. **36**, 1263 (1976); C.H. Chang, Nucl. Phys. **B172**, 425 (1980); E.L. Berger and D.L. Jones, Phys. Rev. D **23**, 1521 (1981); R. Baier and R. Ruckl, Nucl. Phys. **B201**, 1 (1982).
- [2] R. Barbieri, M. Caffo, R. Gatto, and E. Remiddi, Phys. Lett. B **95**, 93 (1980); Nucl. Phys. **B192**, 61 (1981).
- [3] R. Barbieri, R. Gatto, and E. Remiddi, Phys. Lett. B **61**, 465 (1976).
- [4] F. Abe *et al.* (CDF Collaboration), Phys. Rev. Lett. **69**, 3704 (1992); **71**, 2537 (1993); **79**, 572 (1997); **79**, 578 (1997).
- [5] G. T. Bodwin, E. Braaten, and G. P. Lepage, Phys. Rev. D **51**, 1125 (1995); **55**, 5853(E) (1997).
- [6] G. T. Bodwin, E. Braaten, and G. P. Lepage, Phys. Rev. D **46**, R1914 (1992).
- [7] E. Braaten and S. Fleming, Phys. Rev. Lett. **74**, 3327 (1995); E. Braaten and T.C. Yuan, Phys. Rev. D **52**, 6627 (1995).
- [8] N. Brambilla *et al.*, arXiv:hep-ph/0412158; J. P. Lansberg, Int. J. Mod. Phys. A **21**, 3857 (2006); J. P. Lansberg *et al.*, AIP Conf. Proc. **1038**, 15 (2008).
- [9] J. P. Ma, B. H. J. McKellar, and C. B. Paranaivitane, Phys. Rev. D **57**, 606 (1998); G. Japaridze and A. Tkabladze, Phys. Lett. B **433**, 139 (1998); R.M. Godbole, D. Indumathi, and M. Kramer, Phys. Rev. D **65**, 074003 (2002); C.F. Qiao, Phys. Rev. D **64**, 077503 (2001); B. A. Kniehl, C. P. Palisoc, and L. Zwirner, Phys. Rev. D **66**, 114002 (2002); M. Klasen, B. A. Kniehl, L. N. Mihaila, and M. Steinhauser, Phys. Rev. D **68**, 034017 (2003); P. Artoisenet, F. Maltoni, and T. Stelzer, J. High Energy Phys. 02 (2008) 102.
- [10] M. Klasen, B. A. Kniehl, L. Mihaila, and M. Steinhauser, Nucl. Phys. **B609**, 518 (2001).
- [11] M. Klasen and J. P. Lansberg, Nucl. Phys. B, Proc. Suppl. **179-180**, 226 (2008).
- [12] S. Todorova-Nova, *31st International Symposium on Multiparticle Dynamics (ISMD 2001), Datong, China, 2001*, arXiv:hep-ph/0112050; J. Abdallah *et al.* (DELPHI Collaboration), Phys. Lett. B **565**, 76 (2003).
- [13] M. Klasen, B. A. Kniehl, L. N. Mihaila, and M. Steinhauser, Phys. Rev. Lett. **89**, 032001 (2002).
- [14] A. V. Lipatov and N. P. Zotov, arXiv:hep-ph/0304181; O. J. P. Eboli, E. M. Gregores, and J. K. Mizukoshi, Phys. Rev. D **68**, 094009 (2003); A. V. Lipatov and N. P. Zotov, Eur. Phys. J. C **41**, 163 (2005); B. A. Kniehl, D. V. Vasin, and V. A. Saleev, Phys. Rev. D **73**, 074022 (2006).
- [15] M. Klasen, B. A. Kniehl, L. N. Mihaila, and M. Steinhauser, Nucl. Phys. **B713**, 487 (2005); Phys. Rev. D **71**, 014016 (2005).
- [16] P. L. Cho and A. K. Leibovich, Phys. Rev. D **54**, 6690 (1996); F. Yuan, C. F. Qiao, and K. T. Chao, Phys. Rev. D **56**, 321 (1997); S. Baek, P. Ko, J. Lee, and H. S. Song, J. Korean Phys. Soc. **33**, 97 (1998); K. Y. Liu, Z. G. He, and K. T. Chao, Phys. Rev. D **68**, 031501 (2003); **69**, 094027 (2004); Z. G. He, Y. Fan, and K. T. Chao, Phys. Rev. D **75**, 074011 (2007).
- [17] Y. J. Zhang and K. T. Chao, Phys. Rev. Lett. **98**, 092003 (2007); B. Gong and J. X. Wang, arXiv:0904.1103.
- [18] C. F. Qiao and J. X. Wang, Phys. Rev. D **69**, 014015 (2004).
- [19] P. Artoisenet, J. P. Lansberg, and F. Maltoni, Phys. Lett. B **653**, 60 (2007); K. Hagiwara, W. Qi, C. F. Qiao, and J. X. Wang, arXiv:0705.0803; P. Artoisenet, *9th Workshop on Non-Perturbative Quantum Chromodynamics, Paris, France, 2007*, p. 21.
- [20] S. P. Baranov, Phys. Rev. D **73**, 074021 (2006); **74**, 074002 (2006).
- [21] E. L. Berger and D. L. Jones, Phys. Lett. B **121**, 61 (1983).
- [22] K. Abe *et al.* (Belle Collaboration), Phys. Rev. Lett. **89**, 142001 (2002).
- [23] J. H. Kuhn, J. Kaplan, and E. G. O. Safiani, Nucl. Phys. **B157**, 125 (1979); R. Baier and R. Ruckl, Z. Phys. C **19**, 251 (1983); B. Humpert, Phys. Lett. B **184**, 105 (1987).
- [24] J. Kublbeck, M. Bohm, and A. Denner, Comput. Phys. Commun. **60**, 165 (1990); T. Hahn, Comput. Phys. Commun. **140**, 418 (2001).
- [25] R. Mertig, M. Bohm, and A. Denner, Comput. Phys. Commun. **64**, 345 (1991).
- [26] E. J. Williams, Phys. Rev. **45**, 729 (1934); C. F. von Weizsacker, Z. Phys. **88**, 612 (1934); S. Frixione, M. L. Mangano, P. Nason, and G. Ridolfi, Phys. Lett. B **319**, 339 (1993).
- [27] I. F. Ginzburg, G. L. Kotkin, V. G. Serbo, and V. I. Telnov, Nucl. Instrum. Methods Phys. Res. **205**, 47 (1983).
- [28] V. I. Telnov, Nucl. Instrum. Methods Phys. Res., Sect. A **294**, 72 (1990).
- [29] M. Gluck, E. Reya, and I. Schienbein, Phys. Rev. D **60**, 054019 (1999); **62**, 019902(E) (2000).
- [30] M. Gluck, E. Reya, and A. Vogt, Eur. Phys. J. C **5**, 461 (1998).
- [31] Jian-Xiong Wang, private communications. In Ref. [18] there was a minor error in the photon spectra function that was used.